

This item was submitted to Loughborough's Institutional Repository (<https://dspace.lboro.ac.uk/>) by the author and is made available under the following Creative Commons Licence conditions.



For the full text of this licence, please go to:
<http://creativecommons.org/licenses/by-nc-nd/2.5/>

Modeling of vegetated rivers for inbank and overbank flows

K. Shiono¹

Loughborough University, Loughborough, Leicestershire, LE11 3TU, UK

M. Takeda²

Chubu University, Kasugai, Aichi, 487 8501, Japan

K. Yang³

SuichanUniversity, Chengdu, Sichuan, 610065, China

Y Sugihara⁴

Kyushu University, Fukuoka, Japan

T. Ishigaki⁵

Kansai University, Suita city, Osaka, 564-8680, Japan

ABSTRACT Model parameters such as friction factor and eddy viscosity in the Shiono & Knight method (SKM) are considered through experimental data obtained from a vegetated open channel. The experiment was conducted in a rectangular open channel with cylindrical rods as vegetation. Velocity, Reynolds stresses and boundary shear stress were measured with Acoustic Doppler Velocimetry (ADV) and a Preston tube respectively. Both friction factor and eddy viscosity were calculated using the measured data and found to be not constant in the shear layer generated by rods. The analytical solutions of SKM to predict velocity and boundary shear stress currently in use were based on the constant assumption of these parameters. In this paper a new analytical solution was derived by taking into account a variation of these parameters and was also verified with the experimental data. This solution was also applied to flow in compound channel with vegetation. The new solution gives a good prediction of the lateral distribution of depth-averaged velocity and boundary shear stress in vegetated channels, and it predicts the boundary shear stress better than that of the original solution without considering the secondary flow term in particular.

1. INTRODUCTION

Flooding is the most common cause of loss of life, human suffering and widespread damage to buildings, crops and infrastructure. However, flooding is a natural and necessary process for the maintenance of the ecology of a river, promoting the exchange of material and organisms amongst a mosaic of habitats. The influence of riparian vegetation on both ecological and hydraulic processes has therefore become increasingly recognized as an integral component of river management. Vegetation such as trees and bushes commonly occurs along the banks of rivers and the edges of floodplains (see Fig.1), both naturally and by design for erosion prevention, habitat creation and landscape. Despite this, there is little known of the effect of such marginal vegetation on flood hydraulic processes, mass exchanges, sediment transport, and pollutant dispersion during river flood. This is thus a key weakness in the application of numerical models in flood risk management and river rehabilitation studies. This paper therefore particularly focuses on the impact of trees and bushes on the key topics of velocity and boundary shear stress.



Fig. 1 One line trees at the edge of Floodplain of flooding river.

Most rivers and man-made channels have floodplains that extend laterally away from the river, forming so-called “compound channels”. Fundamental research on compound channel hydrodynamics was carried out in 1990th and revealed the presence of high levels of turbulence, secondary flows and large horizontal eddies at the junction be-

tween the floodplain and the main channel. The results of this work led to the creation of the Shiono and Knight Method (SKM) for analysis of overbank flows (Shiono & Knight, 1988, 1991). This SKM cannot separate the influence of the drag friction of riparian vegetation from the boundary friction, and Rameshwaran & Shiono, (2007) demonstrated significant over-prediction of boundary shear stress for an emergent vegetation case and then introduced the drag force term in SKM. As a result, the prediction of boundary shear stress was great improvement. In experimental studies, Sun and Shiono, (2009) demonstrated that flow resistance caused by drag force due to such vegetation in a small aspect ratio of open channel is significant. The vegetal drag force thus affects flood water levels and consequently flood hazard maps in a relative small aspect ratio of rivers.

The exchange of momentum is the key to control flow resistance in the vicinity of vegetated areas. Most popular expression of momentum exchange is velocity gradient with eddy viscosity. For SKM, the eddy viscosity is expressed with the bed and rod generated turbulence (Shiono et al 2009), and non dimensional eddy viscosity within the analytical solutions of SKM is assumed to be constant, however the measured non dimensional eddy viscosity (White and Nepf, 2008) in open channel flow with the vegetation tends to show different behaviour to that assumed in the analytical solutions for SKM. The friction factor for SKM is also the key factor and is assumed to be constant. The friction factor however appears to be also not constant in the shear layer region occurred by vegetal drag as shown in Xin and Shiono (2009). Therefore the eddy viscosity and friction factor need to be refined in such region in SKM. In this paper, a new analytical solution is derived based on having a variation of friction factor and non dimensional eddy viscosity. This analytical solution is validated with the measured velocity and boundary shear stress in an open channel with one line vegetation.

2. EXPERIMENT SETUP

Experiments were conducted in a 9m long and 0.915m wide rectangular channel in Loughborough University (LU). A honeycomb was placed at the inlet of the channel to remove large undulations of water surface. A single line of vegetation was made from a series of 9mm diameter wooden rods. These were held in place at $y=0.455\text{m}$ (centre of the channel) with a series of wooden cross members spanning the width of the channel. The centre to centre spacing between the rods was taken as 160mm, which therefore implies a rod spacing ratio L/D of

17.8, (L =rod spacing and D =rod diameter). This is based on the averaged tree spacing along a reach of the River Thames, Terrier, et al (2010). The bed slope, S_0 was set to 0.001, and the water depth was at 0.3m in the measurement area between 4.7m and 5.3m downstream. Because the channel was not long enough for uniform flow to be established, the energy slope was therefore estimated by balancing the forces such as the Reynolds shear force at the rod and boundary shear force and the weight component and was 0.00016. This value is used as the energy slope in this paper.

Data collections were performed using ADV for velocity and a Preston tube for boundary shear stress. For ADV, measurements were carried out at 9 half cross sections over 0.7m length along the channel as shown in Fig. 2. The measurements were taken place at 4 vertical distances with 6 traverse locations for each the half cross section.

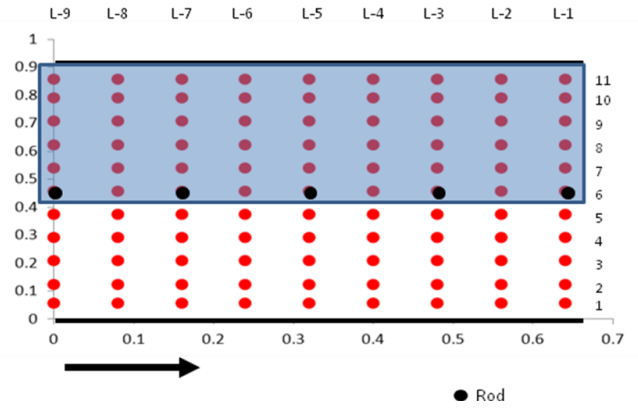


Fig. 2 Measurement locations in the channel

The data recording each point was 3 minutes and the sample data rate was 100Hz. For the Preston tube, the measurements were carried out at the same transverse and longitudinal locations as with the ADV measurements. The data recording length for each location was also 3 minutes.

3. EXPERIMENTAL RESULTS

A typical velocity distribution in the half cross section between rods at 5.2m downstream from the inlet is shown in Fig. 3, (U =longitudinal velocity, z = vertical distance and y =lateral distance). There is a tendency to have slower velocity near the rod and the maximum velocity around the half water depth, which demonstrates a distinct velocity dip as happened in a narrow channel. It can be seen from the figure that there has a tendency of bulging flow in the shear layer near water surface even the velocity

was measured below 0.24m from the water surface. This suggests that the drag force caused by the rods is significant in the water surface area. The transverse component of the Reynolds stress caused by the vertical plane shearing is also shown in Fig. 3, ($\overline{\rho uv}$ =Reynolds stress). A large Reynolds stress occurs near the rod area around $y=0.45\sim 0.55\text{m}$ due to the drag force of the rods. It was noticed that the magnitude of the vertical component of the Reynolds stress caused by the horizontal plan shearing in most area was considerably smaller than transverse component one. There was a tendency of the vertical component to have its largest near bed, which indicates the dominance of bed generated turbulence, however the transverse component is dominated over the water depth near the rod area.

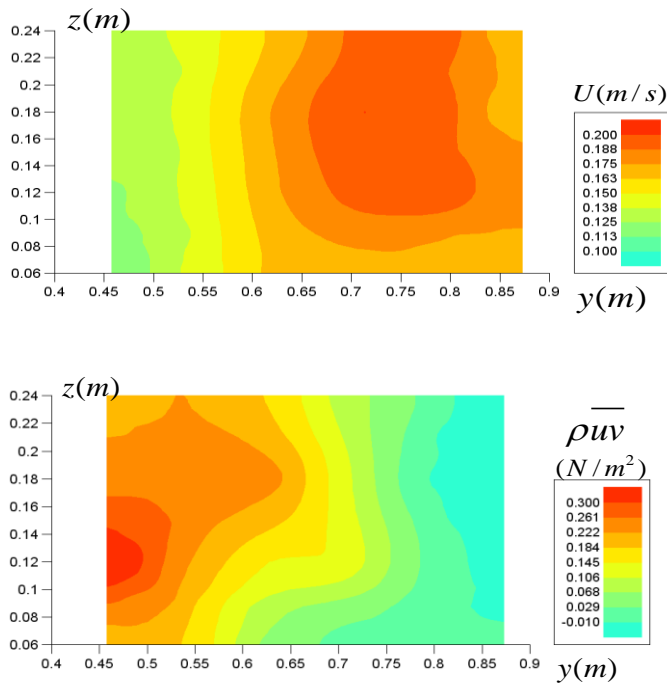


Fig. 3 Velocity and Reynolds stress distributions

Depth averaged velocities in the measurement sections were estimated using available data and are shown in Fig. 4 including the transverse component of the depth averaged Reynolds stress and the boundary shear stress. The transverse component of the depth averaged Reynolds stress in the measurement sections included in Fig. 4 was calculated using those values of 9 cross sections along the channel. It can be seen from the figure that there is a maximum velocity at a distance of 1/3 width from the channel wall ($y=0.9\text{m}$) and the Reynolds stress apparently varies linearly within the half cross section in the channel. This suggests that the drag force caused by the rods is almost 2 times the wall shear force.

It is noticed that the location of zero of the Reynolds stress is not corresponding to the location of the maximum velocity. They should be coincided but not in this experiment. This may be due to a lack of measurement points.

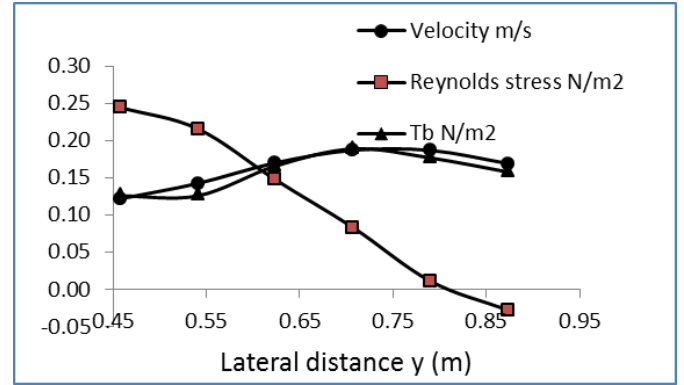


Fig. 4 Depth averaged velocity and Reynolds stress and Boundary shear stress, and

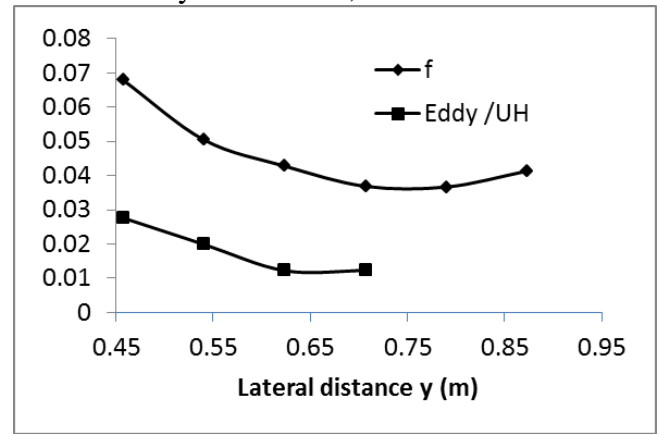


Fig. 5 Friction factor and eddy viscosity/(UH).

The distribution of boundary shear stress (Tb) has a trend similar to that of the depth averaged velocity as shown in Fig. 4. The boundary shear stress is proportional to velocity squared near the bed, and as can be seen in Fig. 3, there is a tendency of the distribution of velocity near the bed similar to the boundary shear stress distribution. The Darcy and Weisbach friction factor (f) that is one of key parameters in SKM was worked out using the depth averaged velocity and boundary shear stress, and are plotted on Fig. 5. The friction factor appears to be constant from the wall ($y=0.9\text{m}$) to $y=0.7\text{m}$ and then linearly increases to the rod. It seems to have the linear variation of the friction factor in the shear layer generated by the rods ($y=0.45\text{m}$). This identification of the linear and constant variations is important when we revisit SKM considering friction factor. The analytical solution of SKM currently assumes a constant friction factor, which means that the linear variation of the friction factor in the shear layer induced by the rods does not support the analytical so-

lution. Thus the assumption of friction factor for the analytical solution of SKM needs to be reconsidered.

The depth averaged eddy viscosity which is also one of the key parameters in SKM was calculated using the depth averaged Reynolds stress and the depth averaged velocity gradient. The depth averaged velocity gradient was obtained by fitting the third order polynomial on the depth averaged velocity. As mentioned in the previous section that the Reynolds stress is not zero at the velocity gradient equal to zero (i.e. at the maximum velocity around 0.77), the eddy viscosity becomes infinity at the maximum velocity. We avoided at around $y=0.77\text{m}$ to work out the eddy viscosity and only calculated it in the shear layer from the rod to near the maximum velocity. The eddy viscosity was divided by UH (U =depth averaged velocity and H =water depth) and then was plotted in Fig. 5. The division of UH is directly related to the SKM analogy, which will be described in next section. The maximum value of non-dimensional eddy viscosity, eddy/ u^*H , was 0.164 which is much larger than that of bed generated turbulence, a typical value of eddy/ u^*H is 0.07. u^* is the friction velocity. The eddy viscosity increases from $y=0.6\text{m}$ towards the rod in the shear layer, which means that it does not support the constant assumption of the eddy viscosity in SKM. This parameter in SKM needs to be also reconsidered.

4. DERIVATION OF ANALYTICAL SOLUTIONS

Lateral distribution methods to predict depth averaged velocity and boundary shear stress in open channel flow have been proposed, for example, by Shiono and Knight (1988, 1991), van Prooijen et al, (2005). The model considered in this paper is the Shiono and Knight Method (SKM) developed by Shiono and Knight (1991). SKM including drag force induced by vegetation is given by Rameshwaran and Shiono (2007) and Shiono et. al. (2009). This solves the second order differential equation for uniform flow:

$$\begin{aligned} \frac{\partial}{\partial y} [H(\rho \overline{UV})_d] &= \rho g S_f H - \tau_b \\ + \frac{\partial (H \overline{\tau_{yx}})}{\partial y} - F_D \end{aligned} \quad (1)$$

where x , y are the longitudinal, and lateral directions respectively, U_d and V_d is the depth-averaged velocities in the x and y directions respectively, ρ is the density of water, g is the gravitational acceleration,

S_f is the energy slope and F_D is the source term; τ_b is the bed shear stress, H is the local water depth.

The bed shear stress (τ_b) and the depth-averaged Reynolds shear stress ($\overline{\tau_{yx}}$) can be determined from the following Equation 2:

$$\begin{aligned} \tau_b &= \frac{f}{8} \rho U_d^2 & \overline{\tau_{yx}} &= \rho \overline{\varepsilon_t} \frac{dU_d}{dy} \\ \overline{\varepsilon_t} &= \overline{\lambda_{tb}} \left(\frac{f}{8} \right)^{\frac{1}{2}} UH(y) \end{aligned} \quad (2)$$

where f is the local friction factor, $\overline{\varepsilon_t}$ is the depth-averaged eddy viscosity, and $\overline{\lambda_{tb}}$ is the depth-averaged dimensionless eddy viscosity.

For no rod area, the source term F_D is zero. For the rod area as vegetation, the source term F_D is drag force per unit area and given by:

$$F_D = \frac{1}{2} \rho N C_D S_F D H U_d^2 \quad (3)$$

N = the total rod number/unit area, D =rod diameter, S_F =shading factor and C_D =drag coefficient.

Substituting equation (2) in equation (1) gives

$$\begin{aligned} \rho g H S_f - \rho \frac{f}{8} U_d^2 + \rho \frac{\partial}{\partial y} \left\{ \lambda H^2 \sqrt{\frac{f}{8}} \frac{1}{2} \frac{dU_d^2}{dy} \right\} - F_D \\ = \frac{d}{dy} \{ H(\rho \overline{UV})_d \} \end{aligned} \quad (4)$$

Assuming that f , λ and advection term are constant in a constant water depth domain, Shiono et.al (2009) derived an analytical solution to equation (4) as

$$U_d^2 = A_1 e^{\gamma y} + A_2 e^{-\gamma y} + \frac{g S_0 H}{\left(\frac{f}{8} + \frac{1}{2} N C_D D H \right)} (1 - \beta) \quad (5)$$

where

$$\begin{aligned} \gamma &= \left\{ \frac{\left(\frac{f}{8} + \frac{1}{2} N C_D D H \right)}{\frac{\lambda}{2} \sqrt{\frac{f}{8}} H^2} \right\}^{1/2} & \beta &= \frac{\Gamma}{\rho g S_0 H} \\ \Gamma &= \frac{dH(\rho \overline{UV})_d}{dy} \end{aligned} \quad (6)$$

Rameshwaran and Shiono (2007) solved equation (4) numerically, rather than analytically.

As can be seen in Fig. 5 that the friction factor and the eddy viscosity are not constant in the shear layer, the above analytical solution cannot be used to solve depth averaged velocity and boundary shear stress in the shear layer region for this experiment case. Because the friction factor appears to vary linearly, it is therefore proposed that the friction factor within the shear layer varies linearly as a first approximation in order to obtain an analytical solution of SKM.

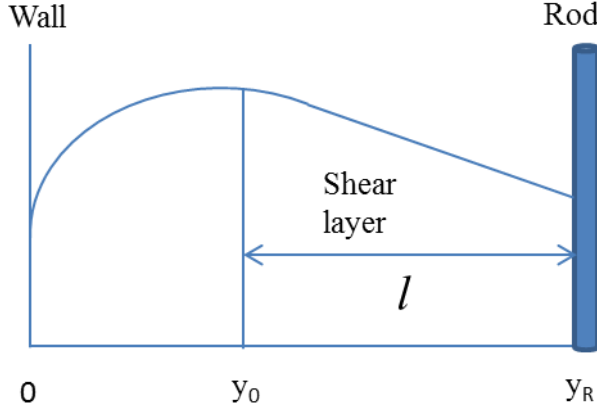


Fig. 6 Sketch of shear layer with rod

The friction factor is now set in the form: (notations are shown in Fig.6)

$$f = f_0 \xi \quad (7)$$

where

$$\xi = \left[1 - \left(\frac{y - y_0}{l} \right) \left(1 - \frac{f_{\max}}{f_0} \right) \right]$$

l is shear layer width, y_0 is at the outside of the shear layer, f_0 is at $y=y_0$, f_{\max} is at the rod, $y_R=y_0+l$.

This gives a maximum value, f_{\max} at the rod and decreases linearly toward the friction factor f_0 at the outside of the shear layer.

Now let us consider the eddy viscosity term in equation (4) with the linear variation of the friction factor. In order to have an analytical solution of equation (4) the eddy viscosity term should have U times the cubic ξ defined as

$$\bar{\varepsilon}_t = \bar{\lambda} \sqrt{\frac{f_0}{8}} \xi^3 HU \quad (8)$$

One can then obtain the following analytical solution for constant water depth.

$$U_d^2 = A_3 \xi^{\alpha_1} + A_4 \xi^{\alpha_2} + \frac{gHS_0}{\frac{f_0}{8} + D} \xi^{-1} (1 - \beta) \quad (9)$$

where

$$\alpha_1 = -1 + \sqrt{1 + \frac{f_0}{8D}} \quad \alpha_2 = -1 - \sqrt{1 + \frac{f_0}{8D}}$$

$$D = \lambda \sqrt{\frac{f_0}{8}} \frac{J^2 H^2}{2} \quad J = -\left(\frac{1}{l} \right) \left(1 - \frac{f_{\max}}{f_0} \right)$$

The coefficients of A_3 and A_4 can be solved with boundary conditions

5. SOLVING MODEL SOLUTIONS

Equations (5) and (9) give the lateral distributions of depth averaged velocity and boundary shear stress (via equation (2)) in no shear layer region and shear layer region respectively. In this experimental open channel case, the half channel cross section was divided into two subsections consisting of the shear layer induced by the rods and the outside of this shear layer. This leads 4 unknown coefficients, A_1 , A_2 , A_3 and A_4 in equations 5 and 9. In order to solve these coefficients, a system of equation is first made by the boundary conditions assuming the continuity of U_d and dU_d/dy at the joint of the subsections, and it becomes a 4 x 4 system of equation. Microsoft Excel can be used to solve a 4 x 4 system of equation from which all the coefficients A 's are calculated, hence the velocity and boundary shear stress distributions can be worked out by equations (5) and (9).

Let's now consider the friction factor that is required to solve SKM as one of input parameters. Fig. 5 shows that the friction factor in the outside shear layer tends to be constant. In an area of a constant friction factor, Rameshwaran and Shiono (2007) suggested to use the modified Colebrook – White equation as given by Equation 10.

$$f = \left[-2 \log \left(\frac{3.02\nu}{\sqrt{128gH^3 S_f}} + \frac{k_s}{12.30H} \right) \right]^{-2} \quad (10)$$

where ν is the kinematic viscosity of water.

This equation was used to estimate a constant friction factor in the outside of the shear layer in this case. The measured data were used to calibrate the roughness height k_s which was found to be 0.01m. This gives f_0 . In the shear layer, the friction factor is set to a linear variation as with the experimental data as shown in Fig. 5 and is matching the constant friction factor f_0 at the joint between the shear layer and its outside. The maximum friction factor was estimated from the experimental data. The distribution of friction factor using equation (7) and the data are shown in Fig. 7 and both agree reasonably well.

Let's consider another parameter, the eddy viscosity, required in SKM. The eddy viscosity is expressed with equation (8) in the shear layer. Through the calibration of λ undertaken using the data, λ was found to be 0.1 in the shear layer and 0.03 in the outside of shear layer. The distribution of the eddy viscosity of equation (8) divided by UH, is shown in Fig. 8. The data and equation (8) are reasonably in agreement in the shear layer region.

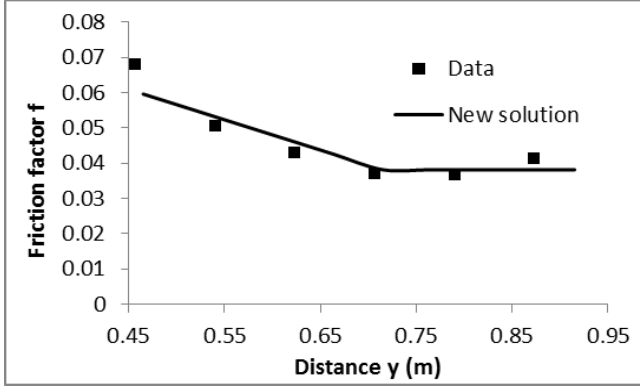


Fig. 7 Distribution of friction factor

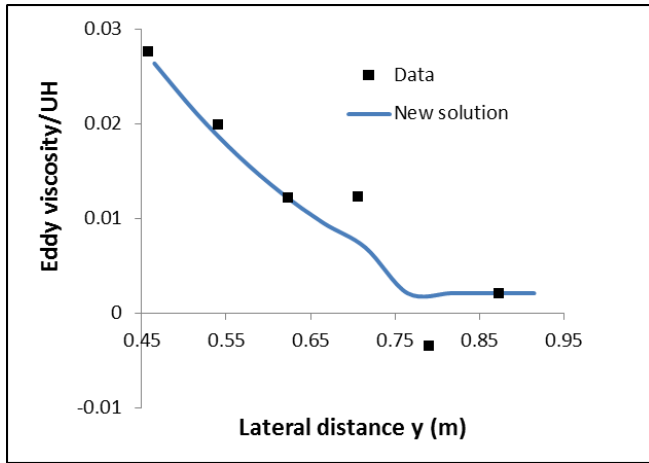


Fig. 8 Distribution of eddy viscosity/UH

6. BOUNDARY CONDITIONS

To solve the analytical solutions in two regions, namely shear layer region and the outside region of the shear layer, the boundary conditions are required at the wall of the channel, the joint of two regions and the rod. At the joint between two regions, conventional the boundary conditions, the continuity and gradient of velocity were used as mentioned in the previous section.

For the boundary condition at the wall, the velocity is usually set to zero. However, this does not give an accurate velocity distribution near the wall, especially in narrow channels. This channel is classified as a narrow channel, and the velocity distribution near the wall using the velocity being set to zero is shown in Fig. 9 as demonstration. To avoid a sharp change

of velocity distribution near the wall and to accurately predict velocity near the wall, the velocity at near the wall for the boundary condition can be assumed to be an appropriate value using either the log-law or the 7th power law. In this case, the velocity at the wall was estimated using the mean boundary shear stress proportion to the wall shear stress with the Darcy friction equation $U^2 = 0.75 RgS_0 / (f/8)$. For the other boundary condition at the rod, the velocity was similarly estimated using the mean boundary shear stress proportional to the drag force/unit area, in this case, $U^2 = RgS_0 / (0.5C_d NHD)$ was used, where $C_d = 1.2$ for the rod. It is noted that these boundary conditions at the wall and rod were only calibrated by the experimental data and an appropriate method is therefore required for establishing boundary conditions at the wall and rod with a variety of data.

With using above the input parameters, namely friction factor and eddy viscosity, and the boundary conditions the predictions of velocity and boundary shear stress were performed with the mathematical solutions (5) and (9) and are shown in Figs. 9 and 10 together with the measured data and the SKM with constant the friction factor and eddy viscosity. It is noted that the secondary flow term was set to zero.

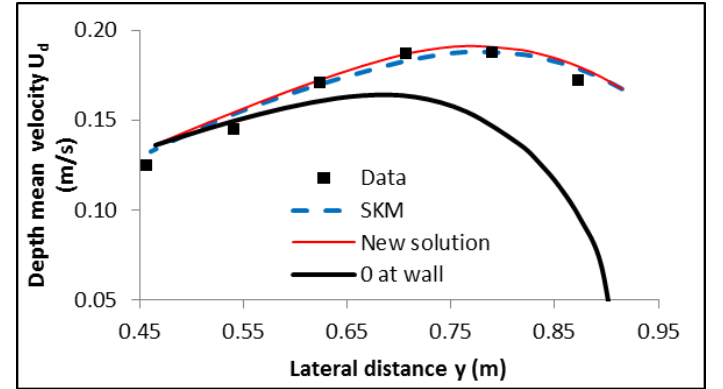


Fig. 9 Predicted and measured velocity.

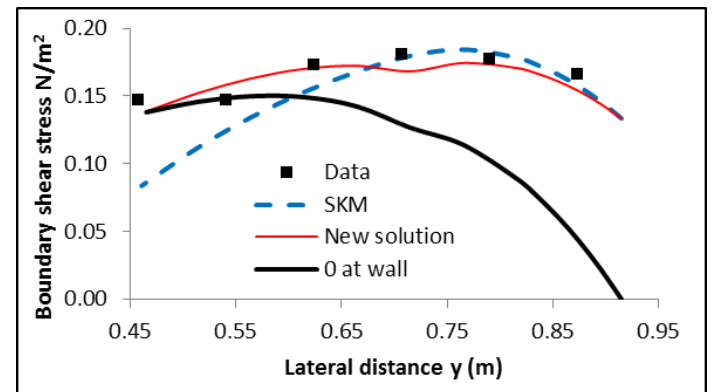


Fig. 10 Predicted and measured boundary shear stress.

The original and new solutions for velocity agree well with the measured data whereas the solutions for the boundary shear stress are quite different in the shear layer. The original SKM solution is under

predicted and this is caused by using the constant friction factor and eddy viscosity in the shear layer albeit both increases towards the rod. It is noticed that there is a slightly dip at the joint between two subsections for the new solution. This is caused by different rates of change of friction factor and velocity as well eddy viscosity. The new solution is now validated with the data.

7. COMPOUND CHANNEL

The new solution was also applied to the compound channel data (Shiono et. al. 2009) and the results are shown in Figs. 11 and 12.

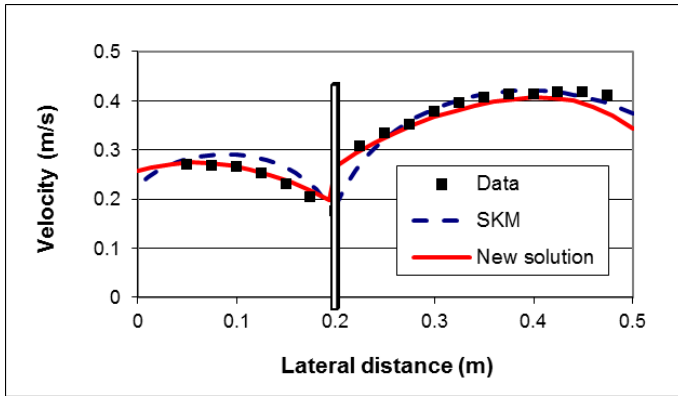


Fig. 11 Measured and Predicted Velocity

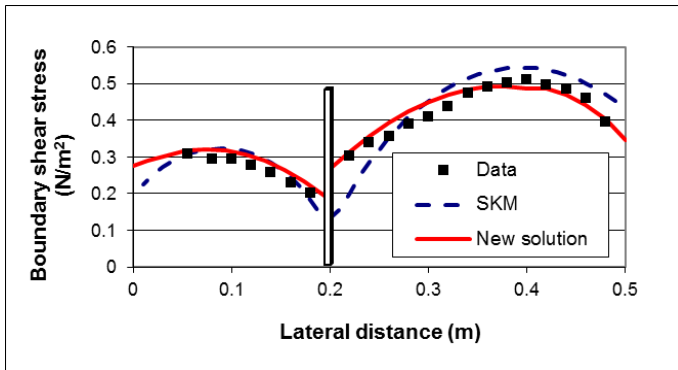


Fig. 12 Measured and predicted boundary shear stress

The compound channel has a series of square rods along the edge of the floodplain and the details of the experimental set up can be found in Shiono et. al. (2009). The SKM in the figures included the secondary flow term $\beta=0.56$, similar to values for cylindrical rods on the floodplain (Rameshwaran and Shiono, 2007, and Xin and Shiono 2008). This is significant high compared with other β values (0.15~0.25) for no rod case (Shiono and Knight (1991). Again the new solution gives a better prediction for the boundary shear stress without the secondary flow term. It should be noted that since the

depth averaged velocity is mathematically discontinuous at the interface between the main channel and floodplain, the prediction was separately undertaken in the main channel and floodplain. The boundary conditions at the main channel and floodplain walls were used as with the simple open channel flow case mentioned above. For floodplain the boundary conditions are $U^2=0.75RgS_0/(f/8)$ at the floodplain wall and $U^2=RgS_0/(0.5C_dNHD)$ at the square blocks. R =hydraulic radius of floodplain. For the main channel, the boundary conditions are $U^2=0.75RgS_0/(f/8)$ at the main channel wall and $U^2=R'gS_0/(0.5C_dNHD)+0.5R'gS_0/(f/8)(h/H)$ which includes the effects of the rod drag force/unit area and the wall shear stress, R' =hydraulic radius of the main channel. It is noted that the constant 0.5 of the wall friction is smaller than a regular value of 0.75 used for the other walls. The shear layer width was estimated from the data in this prediction since there have been no method which determines width of shear layer in the literature except van Prooijen et al, (2005) who introduced shear layer width determined by the concept of percentile of the maximum velocity. In order to establish the method how to determine shear layer width, more data from different channel configurations with different vegetation cases are required.

8. CONCLUSIONS

The experiment was conducted in a single open channel with a series of cylindrical rods, as vegetation, along the centre of the channel. Velocity and Reynolds stress were measured with ADV and boundary shear stress was measured with a Preston tube. The measured velocity, Reynolds stress and boundary shear stress were used to estimate friction factor and eddy viscosity and both were found to be not constant in the shear layer induced by the rods. Based on the experimental data, the variations of friction factor and eddy viscosity in SKM were introduced and a new analytical solution was derived. These variations were a linear function for friction factor and a cubic function for the eddy viscosity in the shear layer. The validation of the new analytical solution was undertaken using two experimental data of the single and two stage channels. With the new analytical solution the predictions of velocity and boundary shear stress are better than those given by the original solution of SKM, and in particular, the prediction of boundary shear stress is much better. The original solution of SKM requires a large value of the secondary flow coefficient, but the new solution does not need to have the secondary flow coefficient because the variation of friction accounts for the secondary flow term. The new solution of SKM can be therefore used to estimate

stage-discharge rating curve and to investigate spacing of trees and bushes for river management.

REFERENCES

- van Prooijen, B.C., Battjes, J.A. and Uijttewaai, W.S.J. (2005). "Momentum Exchange in Straight Uniform Compound Channel Flow". *J. Hydraul. Engrg.* 131, 175–183.
- Rameshwaran, P. and Shiono, K. (2007), Quasi two dimensional model for straight overbank flows through emergent vegetation on floodplains, *JHR*, Vol. 45, No. 3, pp. 302-315.
- Shiono, K. and Knight, D.W., (1988), Two dimensional analytical solution for a compound channel, *Proc. 3 Int. Symp. on Refined Flow Modelling and Turbulence Measurements*, (Editors: Y. Iwasa, N. Tamai and A. Wada), Universal Academy Press, pp.591-599.
- Shiono K. and Knight, D.W. (1991), Turbulent open channel flows with variable depth across the channel, *JFM*, vol. 222, pp.617-646.
- Shiono, K. Ishigaki, T., Kawanaka, R. and Heatlie, F. (2009), Influence of one line vegetation on stage-discharge rating curves in compound channel, 33rd IAHR Congress, Water Engineering for a sustainable Environment, PP1475-1482.
- Sun, X. and K Shiono, K. (2008), Modelling of velocity and boundary shear stress for one-line vegetation along the edge of floodplain in compound channel, *ICHE 2008*, Nagoya, Sept.
- Sun, X. and Shiono, K. (2009), Flow resistance of One-line Emergent Vegetation along the floodplain edge of a Compound Open Channel, *AWR*, vol. 32, pp. 430-438.
- Terrier, B, Ronbinson, S. and Shiono, K, (2010), Influence of vegetation to boundary shear stress in open channel for overbank flow, *Proc. River-flow2010 conference*, Bruansweig, Germany, Vol. 1, pp.285-292.
- White, B.L. and Nepf, H. (2008), Vortex-based model of velocity and shear stress in a partially vegetated shallow channel, *WRR*, vol. 44, pp.1 -15.